# Appendix A

# Counterclockwise Loops in Nyquist Plots

In this appendix, it is shown that a Nyquist plot which contains a counterclockwise loop (such as those in Figures 3.4(d) and (e)) represents a transfer function with at least one RHP pole. Transfer functions of the following form will be considered:

$$A(s) = \frac{\alpha_0 s^m + \alpha_1 s^{m-1} + \cdots + \alpha_m}{s^n + \beta_1 s^{n-1} + \cdots + \beta_n}$$

where $m \leq n$. $N$ will refer to the number of *clockwise* encirclements of the origin by the Nyquist plot of $A(s)$, $P$ to the number of RHP poles of $A(s)$, and $Z$ to the number of RHP zeros of $A(s)$. There are two cases:

**Case 1.** This is the trivial case in which the counterclockwise loop encircles the origin; therefore the Principle of the Argument requires:

$$Z - P = N = -1$$

Clearly, as $Z \geq 0$, it is necessary that $P \geq 1$.

**Case 2.** This is the general case in which the counterclockwise loop does not encircle the origin; therefore:

$$Z - P = 0$$

In this case, we find some point $a+bj$ which is encircled by the loop, and consider a mapping of the Nyquist contour through $A(s) - (a + bj)$. This mapping has a shape identical to that of $A(s)$, but is shifted so that the loop now encircles the origin. Furthermore, it is evident that $A(s)$ and $A(s) - (a + bj)$ share the same poles:

$$A(s) - (a + bj) = \frac{(\theta_0 + \phi_0 j)s^n + (\theta_1 + \phi_1 j)s^{n-1} + \cdots + (\theta_n + \phi_n j)}{s^n + \beta_1 s^{n-1} + \cdots + \beta_n}$$

For the shifted transfer function, the Nyquist plot reveals:

$$Z' - P = -1$$

where $Z'$ is the number of RHP zeros of $A(s) - (a + bj)$. Thus:

$$P = Z' + 1 \geq 1$$

This completes the proof.

# Appendix B

# The LQG/LTR Design Procedure

This appendix provides a brief overview of the Linear Quadratic Gaussian / Loop Transfer Recovery design procedure, with emphasis on the design of a servo for the two-link manipulator (Section 4.4). The results presented in this appendix are based upon the description of LQG/LTR found in Athans [8].

The LQG/LTR procedure is a servo design technique which essentially provides a prescription for a compensator to invert a multi-input, multi-output plant. The compensator is model-based, as shown in Figure B.1. The expression for the compensator, $K(s)$, is:

$$K(s) = G[(sI - A)^{-1} + BG + HC]^{-1}H \tag{B.1}$$

In this development, we will not be concerned with the effects of modeling errors, so the matrices $A$, $B$, and $C$ in the compensator are assumed to be identical to their counterparts in the plant. A discussion of the robustness of LQG/LTR compensators to modeling errors is provided in [56].

The "control gain matrix", $G$, and "filter gain matrix", $H$, in Figure B.1 are the choice of the designer, and their appropriate selection lies at the heart of the technique. The loop transfer recovery result determines the selection of $G$. This result is as follows: if $H$ is chosen such that the eigenvalues of $A - HC$ lie in the LHP, and if a family of control gain matrices parametrized by $\rho$ (termed $G_\rho$) can be found such that

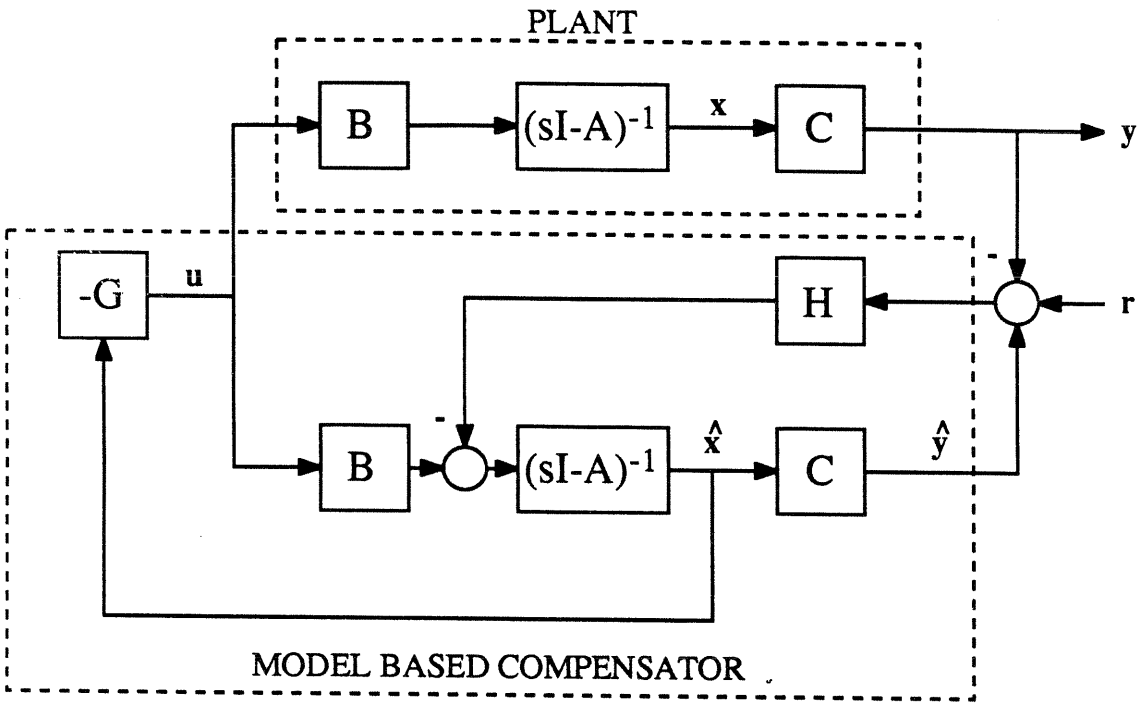


Figure B.1: Structure of the model-based compensator. The matrix $G$ generates a control based upon the state estimate, $\hat{\mathbf{x}}$; the matrix $H$ ensures that the error, $\mathbf{x} - \hat{\mathbf{x}}$, does not diverge.

the eigenvalues of $A - BG_\rho$ lie in the LHP for all $\rho$, and:

$$\lim_{\rho \to 0} \sqrt{\rho} G_\rho \to WC; \quad W'W = I \tag{B.2}$$

then, for each value of $s$, as $\rho \to 0$:

$$T(s) = C(sI - A)^{-1} B K_\rho(s) \to C(sI - A)^{-1} H \tag{B.3}$$

In other words, the behavior of the control system approaches that of the system shown in Figure B.2. The extent to which this "recovery" is effected is a function of $\rho$. Furthermore, such a $G_\rho$ can be found by solving the Control Algebraic Riccati Equation (CARE) for minimum phase, stabilizable $C(sI - A)^{-1}B$:

$$0 = -\Phi_\rho A - A'\Phi_\rho - C'C + \frac{1}{\rho}\Phi_\rho B B' \Phi_\rho \tag{B.4}$$

$$G_\rho = \frac{1}{\rho} B' \Phi_\rho \tag{B.5}$$

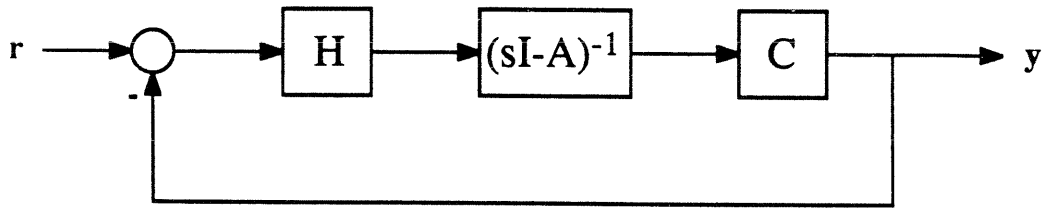


Figure B.2: The "target loop". This is the system which is "recovered" by the loop transfer recovery procedure. It therefore represents the targeted behavior.

It can be shown that $G_\rho$ defined in this manner satisfies the conditon B.2 [8]. An alternative, but less frequently used method of selecting $G_\rho$ is described by Kazerooni [47].

With the LTR result established, the problem becomes one of selecting $H$ to generate a desirable shape for the loop transfer function $C(sI - A)^{-1}H$. One systematic method of selecting $H$ is to use the Filter Algebraic Riccati Equation (FARE) in the following manner:

$$0 = A\Sigma + \Sigma A' + LL' - \frac{1}{\mu}\Sigma C'C\Sigma \tag{B.6}$$

$$H = \frac{1}{\mu}\Sigma C' \tag{B.7}$$

The matrix $L$ and the scalar $\mu$ are now design parameters. $L$ may be used to "shape" the singular values (as functions of frequency) of $C(sI-A)^{-1}H$ (see below), and $\mu$ may be chosen to set the bandwidth.

This completes our brief overview of the procedure, which will now be illustrated with the design of a servo for the two-link manipulator. A block diagram of the servo to be designed is shown in Figure B.3.

The manipulator dynamics are represented by the state matrices $A$ and $B$ (defined in equations 4.1 and 4.2) and the output matrix $C$, which simply selects the velocity

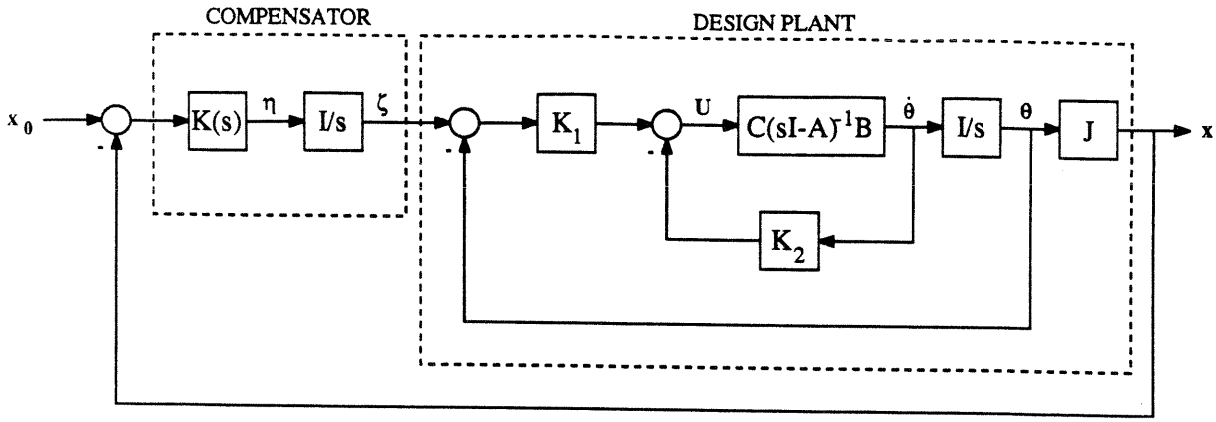


Figure B.3: Block diagram of LQG/LTR controller for the two-link manipulator. Note that this implementation contains integrators in the forward loop.

states, $\dot{\theta}$, as outputs. The position states, $\theta$, can then be found by integrating the velocity, and the endpoint positions can be found from the joint positions through the jacobian matrix, $J$ (recall that this model represents the manipulator behavior only for small excursions about some equilibrium point). The "inner loop" feedback represented by $K_1$ and $K_2$ is intended to condition the manipulator dynamics for the LQG/LTR procedure. All four eigenvalues of $A$ lie very close to the origin of the $s$-plane, a condition which makes the standard approach to selecting $H$ fail. To avoid this difficulty, the eigenvalues are moved into the LHP with $K_1$ and $K_2$. The "design plant" (including the inner loop feedback) has the following state and output equations:

$$\begin{bmatrix} \dot{\theta} \\ \ddot{\theta} \end{bmatrix} = \begin{bmatrix} 0 & 1 \\ -I^{-1}K_1 & I^{-1}(\beta - K_2) \end{bmatrix} \begin{bmatrix} \theta \\ \dot{\theta} \end{bmatrix} + \begin{bmatrix} 0 \\ I^{-1}K_1 \end{bmatrix} \zeta$$

$$\mathbf{x} = \begin{bmatrix} J & 0 \end{bmatrix} \begin{bmatrix} \theta \\ \dot{\theta} \end{bmatrix}$$

This implementation includes an integrator in each forward loop control channel, so that zero steady-state error is achieved. The design plant is augmented with these integrators, and it is the "augmented plant" which is used in the design of the LQG/LTR

compensator. The augmented plant has the following state and output equations:

$$\begin{bmatrix} \dot{\varsigma} \\ \dot{\theta} \\ \ddot{\theta} \end{bmatrix} = \begin{bmatrix} 0 & 0 & 0 \\ 0 & 0 & 1 \\ I^{-1}K_1 & -I^{-1}K_1 & I^{-1}(\beta - K_2) \end{bmatrix} \begin{bmatrix} \varsigma \\ \theta \\ \dot{\theta} \end{bmatrix} + \begin{bmatrix} 1 \\ 0 \\ 0 \end{bmatrix} \eta$$

$$\mathbf{x} = \begin{bmatrix} 0 & J & 0 \end{bmatrix} \begin{bmatrix} \varsigma \\ \theta \\ \dot{\theta} \end{bmatrix}$$

or, in a condensed form:

$$\dot{\xi} = A_a \xi + B_a \eta$$

$$\mathbf{x} = C_a \xi$$

The matrix $H$ is chosen to shape the singular values of the target loop transfer function, $C_a(sI - A_a)^{-1}H$. It can be shown [8] that, if the matrix $L$ in the FARE is chosen as follows:

$$L = \begin{bmatrix} -[C(A - B[\ K_1 \quad K_2\ ])^{-1}B]^{-1} \\ C'[CC']^{-1} \end{bmatrix}$$

the singular values of $C_a(sI - A_a)^{-1}H$ will be "matched" (all have the same magnitude) at low and high frequencies, and that at low and high frequencies, these singular values will drop off at 20 dB/decade as a function of frequency. The targeted loop transfer function, then, is simply a multivariable integrator. The magnitude of this integrator, and therefore the open loop crossover frequency and closed loop bandwidth, may be adjusted with the parameter $\mu$.

Once the target loop has been designed, the matrix $G$ is found by solving the CARE (equation B.5). The parameter $\rho$ is adjusted (decreased) until suitable recovery of the target loop is obtained. The selection of both $\mu$ and $\rho$ must be moderated by attention to the necessary control effort—excessively high bandwidth or close recovery will require excessively large control effort. Step responses of the two-link manipulator were simulated to ensure that the controls were within the capabilities of the hardware.

The complete controller consists of the LQG/LTR compensator, $K(s)$, plus the integrators. Together, these constitute an eighth-order compensator for a fourth order

plant. Such a high-order compensator calls for a digital implementation. Therefore, a discrete time compensator was derived from the contiuous time compensator based upon the first-order approximation, $\mathbf{x}_{k+1} = (1+AT)\mathbf{x}_k + BT\mathbf{U}_k$, where $T$ is the sample period, and $k$ is the discrete time index. The eighth-order discrete time compensator, as implemented, is described by the following state and output equations:

$$\begin{bmatrix} \zeta_{k+1} \\ \mathbf{z}_{k+1} \end{bmatrix} = \begin{bmatrix} 1_{2\times 2} & -GT \\ 0_{6\times 2} & 1_{6\times 6} + (A_a - B_a G - HC_a)T \end{bmatrix} \begin{bmatrix} \zeta_k \\ \mathbf{z}_k \end{bmatrix} + \begin{bmatrix} 0_{2\times 2} & 0_{2\times 2} & 0_{2\times 2} \\ -HT & HJT & 0_{6\times 2} \end{bmatrix} \begin{bmatrix} \mathbf{r}_k \\ \theta_k \\ \dot{\theta}_k \end{bmatrix}$$

$$\mathbf{U}_k = \begin{bmatrix} K_1 & 0_{2\times 6} \end{bmatrix} \begin{bmatrix} \zeta_k \\ \mathbf{z}_k \end{bmatrix} + \begin{bmatrix} 0_{2\times 2} & -K_1 & -K_2 \end{bmatrix} \begin{bmatrix} \mathbf{r}_k \\ \theta_k \\ \dot{\theta}_k \end{bmatrix}$$

The performance of this controller is described in Sections 4.4 and 5.4.4.

# Appendix C

# An Example of Passive Physical Equivalent Synthesis

In this appendix, a passive physical equivalent is synthesized. The system of interest is shown in Figure 7.2; the control law is $u = -GF$. The closed loop driving point admittance is:

$$Y(s) = \frac{v(s)}{F(s)} = \frac{s^2 + (1+G)B\frac{2}{M}s + (1+G)K\frac{2}{M}}{\frac{M}{2}s^3 + 2Bs^2 + 2Ks}$$

It is straightforward to generate an equivalent with the Cauer synthesis techniques. The first step is a continued fraction expansion about infinity. The admittance is written in an anticausal form (i.e., as an impedance), and the pole at infinity is removed:

$$\begin{aligned} Z(s) = Y^{-1}(s) &= \frac{M}{2}s + \frac{(1-G)Bs^2 + (1-G)Ks}{s^2 + (1+G)B\frac{2}{M}s + (1+G)K\frac{2}{M}} \\ &= \frac{M}{2}s + Z_1(s) \end{aligned}$$

This result may be interpreted to mean that a mass, $M/2$, has a common velocity with the rest of the system, represented by $Z_1$, and that the sum of the forces on the mass and $Z_1$ is equal to the force imposed by the environment. A bond graph representation of this result is shown in Figure C.1(a).

The next step is continued fraction expansion about zero. $Z_1$ is inverted, and the

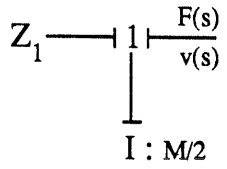


(a)

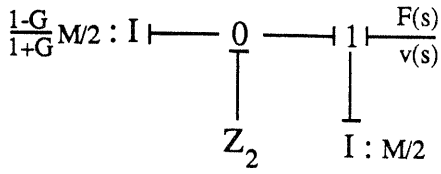


(b)

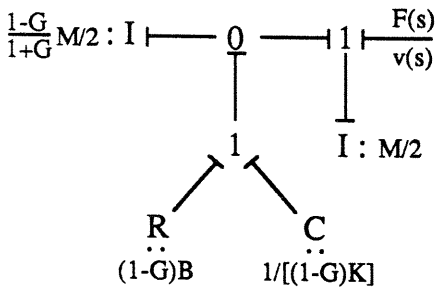


(c)

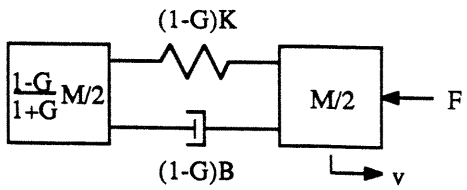


(d)

Figure C.1: Synthesis of a passive physical equivalent. (a) Step 1. (b) Step 2. (c) Bond graph model of complete realization. (d) Mechanical element model of complete realization.

pole at zero is removed:

$$\begin{aligned} Y_1(s) = Z_1^{-1}(s) &= \frac{1+G}{1-G}\frac{2}{Ms} + \frac{s}{(1-G)Bs + (1-G)K} \\ &= \frac{1+G}{1-G}\frac{2}{Ms} + Y_2(s) \end{aligned}$$

The bond graph model, updated to reflect this cycle, is shown in Figure C.1(b).

As a final step, $Y_2$ can be written in impedance form, and a pole at zero can be removed to reveal the contributions of a spring and a damper:

$$Z_2(s) = Y_2^{-1}(s) = (1-G)B + \frac{(1-G)K}{s}$$

A bond graph of the complete realization is shown in Figure C.1(c), and a mechanical element drawing is shown in Figure C.1(d).

# Appendix D

# Preservation of Relative Order

The purpose of this appendix is to show that state and input feedback do not change the relative order of a system's driving point impedance, or the behavior of this impedance at high frequency. The system under consideration is described as follows:

$$\begin{aligned} \dot{\mathbf{x}} &= A_{n\times n}\mathbf{x} + B\mathbf{u} + L\mathbf{e} \\ \mathbf{f} &= C\mathbf{x} \end{aligned}$$

where $\mathbf{u}$ is the control and $\mathbf{e}$ and $\mathbf{f}$ are power duals. It is also assumed that the control ports and interaction ports are non-colocated; the reason for this assumption will become clear in the sequel.

To begin, consider the zeros of the open loop ($\mathbf{u} = 0$) driving point admittance (or impedance). The zeros of the admittance function relating the $i^{th}$ input ($e_i$) to the $j^{th}$ output ($f_j$) are the roots of:

$$Y_{ij} = C_j(sI - A)^{-1}L_i = 0$$

where $C_j$ is the $j^{th}$ row of $C$, and $L_i$ is the $i^{th}$ column of $L$. Consider now $(sI - A)^{-1}$, which may be written in terms of the elements of $A$:

$$(sI - A)^{-1} = \begin{bmatrix} s - a_{11} & -a_{12} & \cdots & -a_{1n} \\ -a_{21} & s - a_{22} & & \\ \vdots & & & \\ -a_{n1} & & & s - a_{nn} \end{bmatrix}^{-1}$$

$$= \frac{1}{\det(sI-A)} \begin{bmatrix} M(s-a_{11}) & -M(-a_{21}) & \cdots & (-1)^{n+1}M(-a_{n1}) \\ -M(-a_{12}) & M(s-a_{22}) & & \\ \vdots & & & \\ (-1)^{n+1}M(-a_{1n}) & & & M(s-a_{nn}) \end{bmatrix}$$

where $M(\xi)$ is the determinant of the minor matrix found by eliminating from $A$ the row and column in which $\xi$ resides. If $\xi = s - a_{ii}$, the minor matrix has only one term containing an $s$ eliminated (namely, $s - a_{ii}$), and $M$ is a polynomial in $s$ of order $n-1$. If $\xi = -a_{ij}$ $(i \neq j)$, two terms containing $s$ are eliminated, and $M$ is a polynomial in $s$ of order $n-2$. Thus, we may write:

$$(sI-A)^{-1} = \frac{1}{\det^{(n)}} \begin{bmatrix} M_{11}^{(n-1)} & -M_{21}^{(n-2)} & \cdots & (-1)^{n+1}M_{n1}^{(n-2)} \\ -M_{12}^{(n-2)} & M_{22}^{(n-1)} & & \\ \vdots & & & \\ (-1)^{n+1}M_{1n}^{(n-2)} & & & M_{nn}^{(n-1)} \end{bmatrix}$$

where the superscripts in parentheses refer to the order of the polynomial. We also note that each of the terms $M_{ii}^{(n-1)}$ is of the form $s^{n-1} + m_{n-2}s^{n-2} + \cdots + m_0$, where the leading coefficient $(m_{n-1})$ is unity.

Our goal is to determine the number of zeros of $Y_{ij}(s)$ and, therefore, the relative order of $Y_{ij}(s)$. In particular, for reasons which will soon be evident, we wish to show that each admittance $Y_{ii}(s)$ contains $n-1$ zeros. To do this, it is necessary to show that $Y_{ii}(s)$ is of the form $y_{n-1}s^{n-1} + y_{n-2}s^{n-2} + \cdots + y_0$, where $y_{n-1} \neq 0$.

To simplify the task of demonstrating that $y_{n-1} \neq 0$, we note that the off-diagonal terms of the matrix above all have order $n-2$, and cannot affect $y_{n-1}$. Thus, we may write:

$$\begin{aligned} \text{L.C.}\{\text{numerator } Y_{ij}(s)\} &= \text{L.C.}\left\{ C_j \begin{bmatrix} s^{n-1}+\cdots & 0 & \cdots & 0 \\ 0 & s^{n-1}+\cdots & & \\ \vdots & & & \\ 0 & & & s^{n-1}+\cdots \end{bmatrix} L_i \right\} \\ &= C_j L_i \end{aligned}$$

where L.C.$\{\cdot\}$ refers to the leading coefficient of the argument. It is now evident that the matrix $CL$ is simply the matrix of leading coefficients of the numerators of $Y(s)$.

The state space passivity criterion (equation 2.38) provides some important information about this matrix:

$$\begin{aligned} PL &= C' \\ CL &= CP^{-1}C' \end{aligned}$$

Because $P$ is a PD matrix, it is clear that $CL$ is a PD or PSD matrix. Furthermore, although $C$ may be singular, no row of $C$ will contain all zeros. It follows from an application of Rayleigh's principle [77] that all diagonal elements of $CL$ will be positive. Thus, each diagonal element of $Y(s)$ will have $n$ poles, $n-1$ zeros, and therefore a relative order of 1.

Now consider the zeros of the *transfer function* $G(s) = C(sI-A)^{-1}B$. If the control and interaction ports were colocated, we would expect to reach the same conclusions that we did for $Y(s)$. However, we have assumed that these ports are non-colocated, and the consequence is that the relative order of each element of $G(s)$ must be greater than 1. Consider, for instance, the example in Figure D.1. As indicated by the transfer function, the relative order is 2. The higher relative order makes intuitive sense, as standard sources of non-colocation, e.g. actuator rolloff or transmission dynamics, should add significant attenuation and lag at high frequencies. We might even expect infinite high frequency lag and infinite relative order in real situations. In conclusion, the matrix $CB$, representing the coefficients of the numerator $s^{n-1}$ terms, should be identically zero:

$$CB = 0$$

We are now prepared to consider the effect of a feedback controller on the relative order of the elements of $Y(s)$. Figure D.2 is a block diagram of the controller. $K(s)$ is a matrix of proper transfer functions which represents the combined effects of sensor and compensator dynamics. A state-space representation of $K(s)$ may be written as

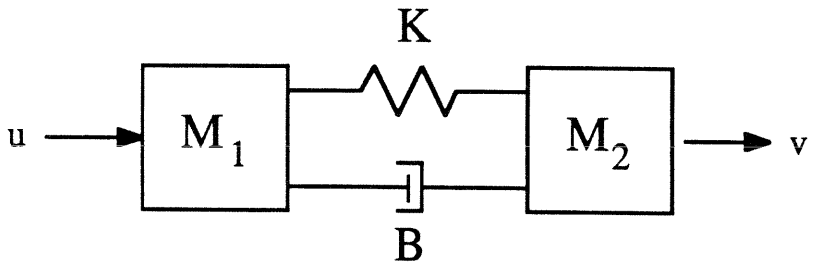


$$G(s) = \frac{v(s)}{u(s)} = \frac{Bs + K}{M_1 M_2 s^3 + (M_1 + M_2)Bs^2 + (M_1 + M_2)Ks}$$

Figure D.1: A system with non-colocated control and interaction ports. The relative order of $G(s)$ is 2.

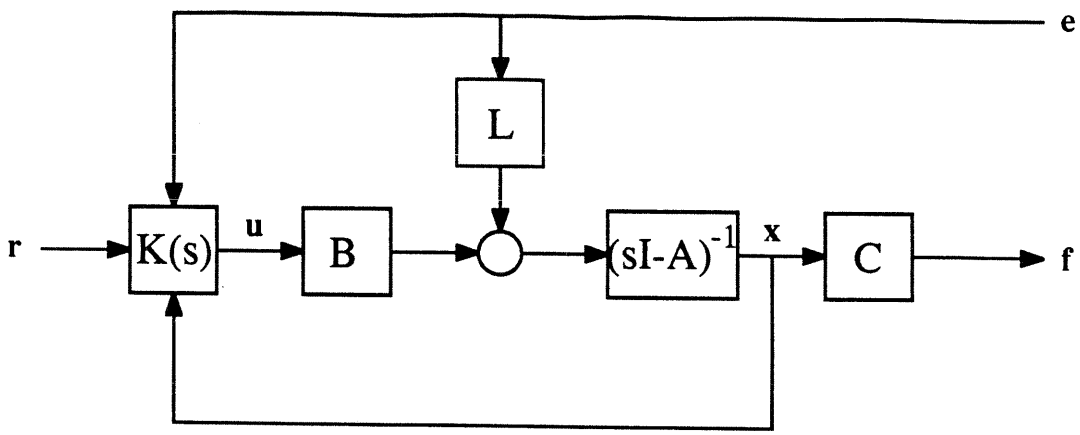


Figure D.2: Block diagram of a general input and state feedback controller with dynamic compensation. The system states are **x**, the control inputs are **u**, the exogenous inputs are **r**, the interaction port inputs are **e**, and the interaction port outputs are **f**.

follows:

$$\begin{aligned}\dot{\mathbf{z}} &= A_K\mathbf{z} + B_{Kx}\mathbf{x} + B_{Ke}\mathbf{e} + B_{Kr}\mathbf{r}, \quad A_K \text{ is } m \times m \\ \mathbf{u} &= C_K\mathbf{z} + D_{Kx}\mathbf{x} + D_{Ke}\mathbf{e} + D_{Kr}\mathbf{r}\end{aligned}$$

where the elements of $\mathbf{z}$ are the sensor and compensator states. The exogenous input, $\mathbf{r}$, will not affect the admittance, and is therefore set to zero. The closed loop state equations are:

$$\begin{aligned}\begin{bmatrix}\dot{\mathbf{x}} \\ \dot{\mathbf{z}}\end{bmatrix} &= \begin{bmatrix}A + BD_{Kx} & BC_K \\ B_K & A_K\end{bmatrix}\begin{bmatrix}\mathbf{x} \\ \mathbf{z}\end{bmatrix} + \begin{bmatrix}L + BD_{Ke} \\ B_{Ke}\end{bmatrix}\mathbf{e} \\ \mathbf{f} &= \begin{bmatrix}C & 0\end{bmatrix}\begin{bmatrix}\mathbf{x} \\ \mathbf{z}\end{bmatrix}\end{aligned}$$

Following the same reasoning as before, the matrix of leading coefficients of the closed loop driving point admittance, $Y_c(s)$, is:

$$\text{L.C.}\{\text{numerator}\, Y_c(s)\} = \begin{bmatrix}C & 0\end{bmatrix}\begin{bmatrix}L + BD_{Ke} \\ B_{Ke}\end{bmatrix}$$

where the leading coefficient now multiplies $s^{n+m-1}$, and the closed loop system is of order $n + m$. Thus:

$$\text{L.C.}\{\text{numerator}\, Y_c(s)\} = CL + CBD_{Ke}$$

But we know that $CB = 0$, so that the leading coefficients are all the same as they were before the control was implemented:

$$\text{L.C.}\{\text{numerator}\, Y_c(s)\} = CL$$

Thus the relative order of $Y(s)$ is unchanged by state or input feedback and, in particular, the relative order of the diagonal terms of $Y(s)$ remains exactly 1.

Because the leading coefficients of the numerator of $Y(s)$ are unchanged by feedback, and the leading coefficients of the denominator are all unity by convention, we have also shown that:

$$\lim_{s\to\infty} Y(s) = \lim_{s\to\infty} Y_c(s)$$

In other words, the high frequency behavior of the closed loop system is identical to that of the open loop system.